Contents lists available at SciOpen

Food Science and Human Wellness

journal homepage: https://www.sciopen.com/journal/2097-0765

China Food Publishing Co.

Anti-hepatocarcinoma effect of polysaccharides extracted from *Lactarius hatsudake* Tanaka mushroom: *in vitro* and *in vivo* studies

Qiao Yang, Songlin Chang, Yiming Tian, Hui Zhang, Feijun Luo, Wang Li*, Jiali Ren*

Hunan Key Laboratory of Forestry Edible Sources Safety and Processing, College of Food Science and Engineering, Central South University of Forestry and Technology, Changsha 410004, China

ARTICLE INFO

Article history:
Received 9 June 2024
Received in revised form 20 July 2024
Accepted 26 August 2024

Keywords:
Lactarius hatsudake Tanaka
Polysaccharide
Anti-hepatocellular carcinoma
In vivo
In vitro

ABSTRACT

Edible mushroom polysaccharides demonstrate a range of bioactivities and have been investigated as potential adjuvant therapies for cancer treatment. Our prior research found *Lactariks hatsudake* Tanaka polysaccharide (LHP) effective against hepatocellular carcinoma, but the mechanisms remain unclear. This study aims to clarify the anti-cancer molecular mechanisms by examining the effects on specific signaling pathways through *in vivo* and *in vitro* analyses. Animal studies showed that LHP significantly inhibited the growth of transplanted liver cancer without toxicity. Histological and immunohistochemical analyses revealed that LHP increased nuclear cohesion in tumor cells and altered the expression of key regulatory proteins such as protein kinase B (Akt), nuclear factor κB (NF-κB), caspase-3, p21, and p53. These findings suggest that LHP's anticancer effects involve promoting apoptosis and disrupting the cell cycle. At the cellular level, assays such as 3-(4,5-dimethylthiazol-2-yl)-5-(3-carboxymethoxyphenyl)-2-(4-sulfophenyl)-2*H*-tetrazolium (MTS), flow cytometry, and transwell invasion confirmed that LHP inhibited cancer cell proliferation and induced apoptosis. Polymerase chain reaction and Western blot assays revealed that LHP intervention reduced cyclin-dependent kinase 4 activity by upregulating p53 and p21, leading to cell cycle arrest and inhibited cell proliferation. LHP also promoted apoptosis by altering Bcl-2-associated X protein, B-cell lymphoma 2, and cleaved caspase-3 levels. Moreover, LHP could affect the Akt, NF-κB, and mitogen-activated protein kinase signaling pathways to exert anticancer effects. These findings underscore the potential of LHP as a novel and multifaceted therapeutic agent. Furthermore, the elucidation of LHP-related mechanisms offers a crucial theoretical foundation for developing innovative and effective treatments for hepatocellular carcinoma. Additionally, this supports its potential development as a functional food or adjuvant therapy for cancer, which holds significant implications and application prospects in both the food and medical fields.

1 Introduction

Cancer incidence and mortality are escalating alarmingly on a global scale, ranking as the leading cause of death across all nations. Statistics revealed that in 2020, approximately 19.3 million new cancer cases were diagnosed, resulting in nearly 10 million deaths worldwide. Projections indicated that this figure will soar to 28.4 million by 2040, marking a startling 47% increase from the 2020 tally[1]. Given this dire situation, there is an urgent necessity for research aimed at identifying more efficacious cancer treatments with reduced adverse effects.

Presently, the primary treatment for cancer methods includes surgery and chemotherapy. However, one significant shortcoming is the recurrence of cancer in some patients, often attributed to drug resistance, tumor cell metastasis, and incomplete surgery[2].

* Corresponding authors at: Central South University of Forestry and Technology, Changsha 410004, China
E-mail address: wli@hnu.edu.cn (W. Li); t20091483@csuft.edu.cn (J.L. Ren)
Peer review under responsibility of Beijing Academy of Food Sciences.

SciOpen Publishing services by Tsinghua University Press

http://doi.org/10.26599/FSHW.2024.9250367

Additionally, the toxicity of chemotherapeutic drugs poses another significant challenge. These drugs lack specificity and can be highly toxic, resulting in varying degrees of harm to both tumor cells and healthy cells concurrently[3]. These results in patients experiencing adverse reactions such as allergies, nausea, vomiting, and other side effects. These side effects would severely compromise a patient's overall health. Consequently, this study is devoted to discovering an effective and non-toxic agent for cancer therapy to alleviate patient suffering and enhance therapeutic outcomes.

In recent years, naturally active polysaccharides have attracted considerable attention within the biomedical field due to their diverse biological activities[4-5]. Particularly as adjuvant therapeutic agents in cancer treatment, these polysaccharides demonstrated reduced toxicity and fewer adverse effects compared to synthetic chemotherapeutics[6-7]. These characteristics improved the safety profile in treatment protocols. Notably, polysaccharides derived from edible mushrooms, recognized for unique biological functions and health-promoting properties and have been extensively utilized in anticancer therapy[8]. Notable examples encompass polysaccharides derived from *Lentinus edodes*[9]. These mushroom polysaccharides have demonstrated efficacy as clinical adjuvants in anticancer drug regimens, thereby offering a promising new avenue for research.

Lactarius hatsudake Tanaka, commonly known as the red milk mushroom, possesses both culinary and medicinal properties. Previous research has highlighted the remarkable ability of *L. hatsudake* Tanaka to effectively inhibit the growth of sarcoma 180 and Ehrlich ascites tumors by more than 90%. Laboratory studies have further demonstrated that *L. hatsudake* Tanaka polysaccharide (LHP) exhibited cytotoxicity against tumor cells *in vitro*. This is possibly due to the presence of *β*-1,3-glucan and galactan structures[10]. These findings provided the potential of LHP as a natural anticancer compound. However, the molecular mechanisms underlying its anticancer effects *in vivo* remain elusive and require further investigation. Previous research has established that polysaccharides possess anticancer properties by specifically targeting critical signaling pathways, particularly the nuclear factor κB (NF-κB) and p53 pathways[11]. The NF-κB pathway is intricately associated with tumor apoptosis, metastasis, and invasion[12]. The p53 pathway is crucial for regulating cell proliferation and apoptosis[13]. These pathways collectively influence the development and progression of cancer cells. Consequently, this study investigated the ability of LHP to exert its anti-hepatocellular carcinoma (HCC) effects through NF-κB and p53 pathways.

Previous studies have demonstrated that LHP exhibits significant cytotoxic effects on HepG2 cells[10]. However, its *in vivo* anticancer activity and underlying mechanisms remain poorly understood. Consequently, the anticancer activity of LHP *in vivo* was evaluated using the HepG2 xenograft model. The mechanisms associated with LHP anticancer by NF-κB and p53 signaling pathways were evaluated through *in vitro* cell experiments. This research laid the precise theoretical foundation for the future application of LHP in anticancer strategies. This study also revealed that LHP is promising for the treatment of HCC.

2 Materials and methods

2.1 Materials

The LHP was isolated from *L. hatsudake* Tanaka fruit bodies referring to the previous method[10]. Briefly, the *L. hatsudake* powder was pretreated with anhydrous ethanol, followed by hot water extraction two times, and obtained the supernatant. The supernatant was then purified by papain, savage method (chloroform: *n*-butanol ratio of 4∶1), dialysis, ethanol alcohol precipitation, and resin adsorption, and finally lyophilized to obtain the LHP solution.

Previous research has purified and yielded LHP with an average molecular weight of 573 kDa. The monosaccharide compositions of LHP were 4.31% mannose, 55.27% glucose, 19.19% galactose, and 7.90% fucose. The chemical compositions of LHP were 79.72% neutral sugar, 3.91% acidic sugar, 5.33% protein, 0.71% phenols, and 7.93% moisture. The LHP was mainly composed of two *α*-1,4-Glc*p*-dominant glucans (LHP-1 and LHP-2), two *α*-1,6-Gal*p*-dominant galactans (LHP-3 and LHP-4) and one *β*-1,3-Glc*p* main chain glucan (LHP-5) composition. The conformation was dominated by spherical aggregates of amorphous flexible fiber chains[10].

The HepG2 cell was obtained from the Cell Culture Center of the Shanghai Institute for Biological Sciences (Shanghai, China). The cultured condition was Dulbecco's modified Eagle's medium (Gibco; NY, USA) with 10% (*V/V*) fetal bovine serum (FBS; NY, USA), 100 U/mL penicillin, and 0.1 mg/mL streptomycin (Gibco; NY, USA) in an incubator (37 ℃, 5% CO_2). 3-(4,5-Dimethylthiazol-2-yl)-5-(3-carboxymethoxyphenyl)-2-(4-sulfophenyl)-2*H*-tetrazolium (MTS) was purchased from Millipore (Shanghai, China). Annexin V and propidium iodide (PI) kits were obtained from BD Pharmaingen (CA, USA). Primary and secondary antibody sources are shown in Table S1. All other chemicals used in this study were of analytical grade.

2.2 Animal model

2.2.1 Design of animal experiment

BALB/c nude specific pathogen-free male mice (4 weeks old, SCXK (Xiang) 2019-0004) were purchased from Hunan Silaikejingda Experimental Animal Co., Ltd. (Changsha, China). All animal procedures were approved by the Laboratory Animal Ethics Committee of Hunan Drug Safety Evaluation and Research Center (HNSE2023(5)031).

To detect the *in vivo* anticancer effects of LHP, the mice were housed under specific pathogen-free conditions (25 ℃, 60% relative humidity, 12 h light/dark cycle), fed, and watered randomly. After acclimatization for 1 week, 0.2 mL HepG2 cells (5×10^6 cells) suspension was inoculated into the axillary subcutis of the right forelimb of all mice[14]. When the average value of the tumors reached 180 mm^3, the mice were divided into 5 groups ($n = 7$). The following treatments were performed: 1) negative control group: 0 mg/kg LHP by gavage daily; 2) low-dose (LHP-L) group: 125 mg/kg LHP by gavage daily; 3) medium-dose (LHP-M) group: 250 mg/kg LHP by gavage daily; 4) high-dose (LHP-H) group: 500 mg/kg LHP by gavage daily; 5) positive control group (cisplatin): 4 mg/kg cisplatin by injection daily (Fig. 1A). The concentration and dosage of LHP based on reference with minor modifications[14]. During the process, body weight and tumor volume (calculated as $V = (a \times b^2)/2$, where a and b are the long and short dimensions (mm^3), respectively) were monitored every 3 days. After 9 days, all mice were sacrificed by cervical dislocation, and samples were photographed and collected for subsequent assays.

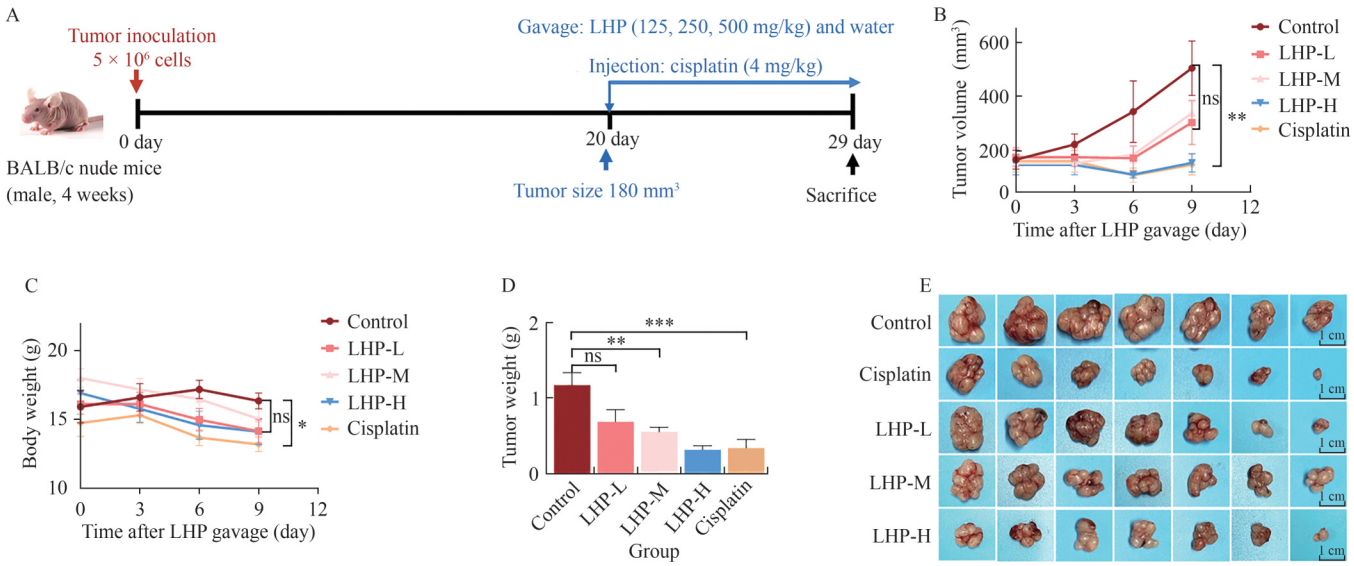

Fig. 1 Inhibitory effects of LHP on tumors *in vivo*. (A) Schematic diagram of animal experiment process; (B) tumor volume, (C) body weight, (D) tumor weight, and (E) tumor images of the mice. The tumor images of mice in each group ($n = 7$) are arranged in descending order of tumor volume (from left to right). Data are presented as mean ± standard error of mean (SEM) of three independent experiments. *** $P < 0.001$, ** $P < 0.01$, * $P < 0.05$, and ns was considered not significant ($P > 0.05$).

2.2.2 *Hematoxylin and eosin (H&E) staining*

The method of H&E staining was referred to in reference[15]. The tumor and liver tissues were fixed in 4% paraformaldehyde, and treated with gradient ethanol and xylene, respectively, to keep the samples dry and transparent. Then, the ultrathin slice (5 μm) obtained with a slicer was stained with H&E reagent after dewaxed in xylene. The stained samples were completed photographed by light microscopy and displayed as color images.

2.2.3 *Histological analysis*

The immunohistochemical assay referred to reported references[16]. Already prepared mouse wax block sections were incubated with the corresponding primary antibody and secondary antibody in sequence. Followed by sequentially staining with a substrate-chromogen solution and hematoxylin. After washing away the unconjugated antibody and with phosphate-buffered saline, the amount of conjugated antibody conjugation was quantified by fluorescence microscopy photographs.

2.3 *Cell model*

2.3.1 *Cell viability and colony formation assay*

MTS was used to detect the survival rates of HepG2 cells after LHP treatment. HepG2 cells were inoculated in 96-well plates and cultured with different concentrations (0, 0.1, 0.2, 0.4, 0.8, 1.6 mg/mL) of LHP solution for 24 h. Subsequently, MTS solution (20 μL) was added to each well at 37 ℃ for 1 h, followed by detecting the absorbance at 490 nm using a microplate reader. All experiments were carried out in triplicate.

To determine the formation of cell colonies, HepG2 cells were incubated with LHP in 6-well plates for 10 days until visible cell colonies appeared. Afterward, the colonies were fixed with 70% (*V/V*) ethanol, stained with 0.1% crystal violet, and counted the colonies.

2.3.2 *Cell cycle assay*

The cell cycle was detected using PI staining. Briefly, HepG2 cells were even incubated in 6-well plates until the cell densities were up to 70%. Then the medium was changed to one containing LHP with various concentrations for 24 h. The treated cells were fixed in refrigerated 70% ethanol overnight. Eventually, prepared cells were reacted with PI in the dark for 10–15 min and then detected by flow cytometry (FACSCanto II; BD, USA).

2.3.3 *Cell apoptosis assay*

PI-Annexin V-fluorescein isothiocyanate double staining assay was used to detect apoptosis. The cells with a density of 70% were cultured with different concentrations of LHP for 24 h. Then reacted with annexin V-fluorescein isothiocyanate (5 μL) and PI (5 μL) for 15 min, followed by detecting the degree of cellular regression using flow cytometry (FACSCanto II; BD, Franklin Lakes, New Jersey, USA).

The apoptotic morphology of HepG2 cells was determined by reference[17]. HepG2 cells were inoculated in 24-well plates and co-cultured with a medium containing LHP for 24 h. Subsequently, the cells were fixed with 70% (*V/V*) ethanol for 5 min at 4 ℃, and quickly stained using Hoechst 33342 or acridine orange/ethidium bromide staining kit (Sangon Biotech (Shanghai) Co., Ltd., Shanghai, China). After washing away the excess dye with phosphate-buffered saline, the cell morphology was observed under a fluorescent inverted microscope (Ti2-E; Nikon, Japan).

2.3.4 *Cell migration assay*

To detect the migratory capacity, HepG2 cells were inoculated in 6-well plates and a line in the middle of each well when

the density reached 90%. Then the HepG2 cells were cultured in an LHP medium for 24 h, and washed with phosphate-buffered saline. The cell density and gap distance were observed under the microscope.

To detect the cell invasive capacity, the serum-starved HepG2 cells were seeded on 24-Transwell culture plates (pore size, 8 μm; Corning Life Sciences, Acton, MA, USA). Further, the medium containing LHP and not was added in the upper chamber and the lower chamber, respectively. After cultured for 24 h, the migrating cells were fixed in formaldehyde, stained with 0.1% crystal violet, and photographed under a microscope to count the number of cells passing through the filters.

2.3.5 Western blot (WB) assay

WB assays were based on previous laboratory procedures[18]. Total proteins were extracted from HepG2 cells treated with LHP (0, 0.1, 0.2, 0.4, 0.8, 1.6 mg/mL). The protein concentration was determined by the BCA protein assay kit (Sangon Biotech, Shanghai, China). The cellular proteins were separated on sodium dodecyl sulfate-polyacrylamide gel electrophoresis (120 V, 30–90 min) in equal amounts, and transferred to polyvinylidene difluoride membranes (60 V, 120 min). The membrane was closed with skimmed milk (5%), incubated with primary antibody at 4 ℃ for 12 h, and incubated with anti-rabbit secondary antibody for 1 h at 25 ℃. After immersing in an electrochemiluminescence luminescent solution, the corresponding protein content was detected by the Bio-Rad imaging system (Bio-Rad, Hercules, CA, USA). The raw data of 3 repetitions of WB are shown in Fig. S1.

2.3.6 Reverse transcription-quantitative polymerase chain reaction (PCR) analysis

The RNA extraction of HepG2 cells was according to the instructions of the Transzol-Up kit (TransGen Biotech, Beijing, China). The quality, purity, and concentration of RNA samples were analyzed by nanodrop ultra microspectrophotometer. The cDNA was synthesized by using a high-performance cDNA reverse transcription kit (TransGen Biotech, Beijing, China) after reaching the standard. The cycling conditions were the following: 94 ℃, initial denaturation for 3 min; 94 ℃, denaturation for 30 s; 60 ℃, annealing for 40 s; 72 ℃, extension for 1 min, and 40 cycles. The relative expression levels of the target genes were calculated by the $2^{-\Delta\Delta Ct}$ method, and the PCR primers are shown in Table S2. The amplification and melt curves are shown in Fig. S2.

2.3.7 Luciferase reporter activity assay

For luciferase reporter activity assay, the HepG2 cells presented in 24-well plates grown by approximately 70%–80% were added to serum-free medium, followed by 1.5 μL Lipo2000 and 1.0 μg activator protein-1 (AP-1) or NF-κB plasmid. After being absorbed for 3 h, the normal medium was replaced with LHP medium and followed by culturing for 12 h, discarding the culture medium, adding cell lysates for 5 min, and collecting the supernatants mixed with luciferase for assay.

2.4 Statistical analyses

The data were from three independent experiments and expressed as mean ± standard deviation (unless otherwise stated). GraphPad Prism 9.0 software was used to analyze the results and significance was calculated by ordinary one-way ANOVA test, followed by Duncan's multiple tests, with $P < 0.05$ indicating a significant difference.

3 Results and discussions

3.1 The inhibitory effect of LHP on the growth of hepatocellular carcinoma in vivo

The anticancer effect of LHP was assayed *in vivo* using a xenograft tumor nude mice mode. The tomor mice mode was established with HepG2 cells. After gavaged of LHP or injection of cisplatin, the tumor growth was inhibited by LHP in a dose-dependent manner. As shown in Figs. 1B, D and E, there was a clear decrease in tumor volume and weight with increasing concentrations of LHP. Specifically, the inhibition rates of low-dose group (125 mg/kg), medium-dose group (250 mg/kg), high-dose group (500 mg/kg), and positive control group (cisplatin of 4 mg/kg) groups were 41.45%, 53.00%, 73.07%, and 74.69%, respectively, after treated for 9 days. These results highlighted the superior anti-tumor effects of the LHP-H group compared to the cisplatin group and glycyrrhiza polysaccharide (56% inhibition at a dose of 500 mg/kg)[19]. The level of toxicity assessment for anticancer drugs is critical[20]. The body weight growth curve, serving as a body health indicator, showed a significant decrease only in the cisplatin group (Fig. 1C). These results indicated that LHP exhibited minimal toxicity compared to the cisplatin group. LHP was evidenced to a category of safe and non-toxic natural products with anticancer activity. The tumor and liver tissue were observed by H&E staining to gain insights into the structural and morphological changes. Following LHP and cisplatin treatment, apoptosis tumor cells presented shrinkage of nuclei. In contrast, the negative control group revealed that the structures of tumor cells were intact and orderly arranged. These results showed that LHP might promote the apoptosis of tumor cells as well as cisplatin (Fig. 2A). Notably, there were no significant morphological or structural changes in the liver tissues across all groups (Fig. 2B), indicating that LHP treatment did not cause systemic damage to liver tissues in mice.

To initially explore the potential molecular mechanisms of LHP anticancer, an immunohistochemical analysis was conducted to assess the expression of p53 and NF-κB pathway-related proteins. The results showed that LHP and cisplatin upregulated the expression levels (brown particles represent positive cells with corresponding antibodies) of p53, p21, and cleaved caspase-3 while downregulated the expression of phospho-protein kinase B (Akt) and phospho-NF-κB compared to the control group (Fig. 2C). These results indicated that LHP had the potential to modulate the p53 and NF-κB signaling pathways, thereby inhibiting tumor growth *in vivo*. The p53 and NF-κB pathways collectively regulate the proliferation, apoptosis, and metastasis of cancer cells. For instance, previous reports indicated that curcumin and hydrazinocurcumin could inhibit HCC growth by phosphatidylinositol-3-kinase (PI3K)/Akt pathway[16,21]. *Lachnum* sp. polysaccharide also could exert anticancer efficiency resulting in p53 activation and NF-κB inhibition[22]. Based on these findings, further

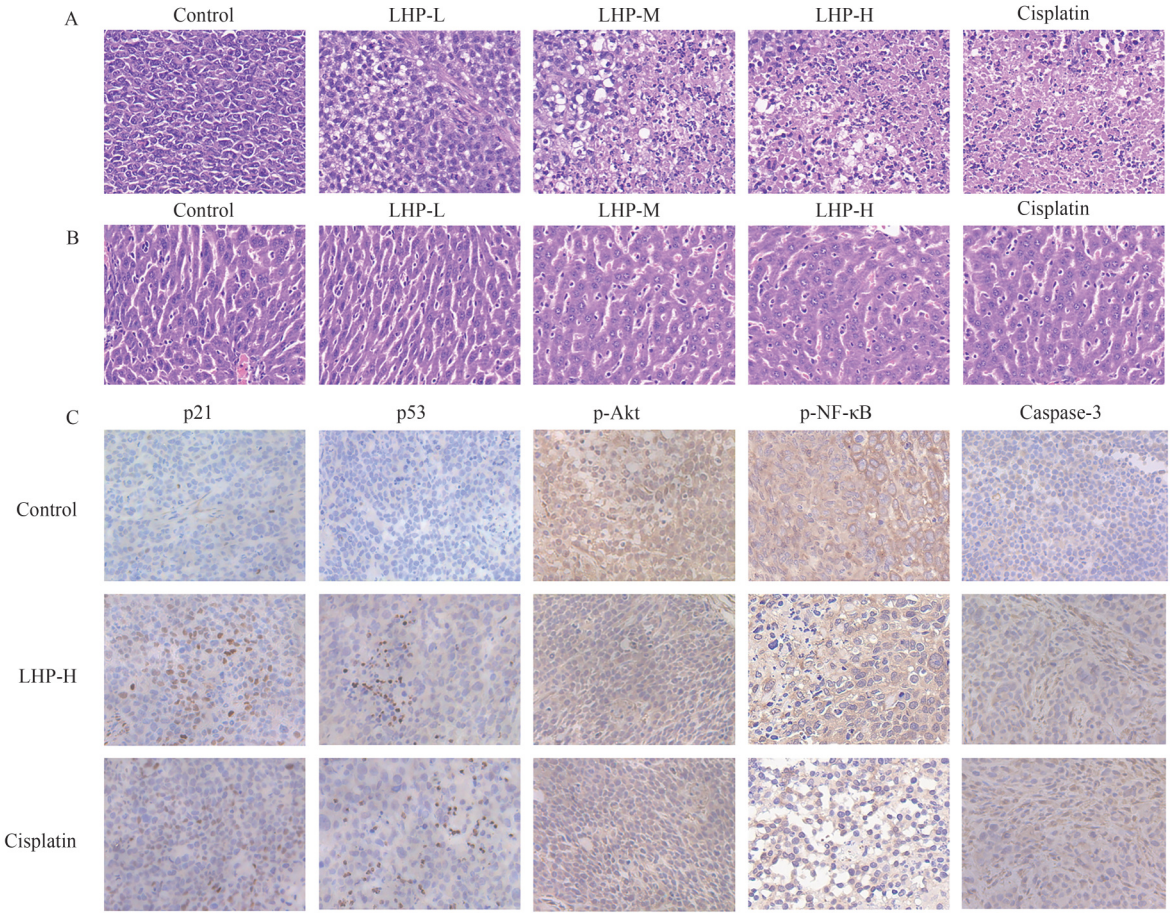

Fig. 2 H&E staining images of (A) tumor and (B) liver tissues. (C) Immunohistochemistry experiment results of p53 and NF-κB pathway-related protein expression. p-NF-κB, phospho-NF-κB; p-Akt, phospho-Akt.

investigation was warranted to determine the anticancer mechanism. Specifically, whether LHP specifically targeted and interfered with p53 and NF-κB pathways to exert its anti-HCC effects.

3.2 The inhibitory effect of LHP on the proliferation of HepG2 cell

Given the high complexities and limited controllability associated with animal models, further and deeper investigation of the LHP anticancer molecular mechanisms was delved[23-24]. Infinite proliferation is one of the important developmental features of tumor cells[25-26]. Therefore, the inhibitory effect of LHP on HepG2 cell proliferation *in vitro* was examined using MTS. Our findings revealed a dose-dependent suppressive effect of LHP on HepG2 proliferation, with a cell survival rate was 61.94% at a concentration of 1.6 mg/mL, as shown in Figs. 3A and B. The antiproliferative ability of LHP was further explored by a colony assay. The results determined a reduction in the number of colonies, with a relative colony formation rate of 53.77% at 1.6 mg/mL LHP (Figs. 3C and D). These findings suggested that LHP could inhibit the proliferation of HepG2 cells.

The cancer cells with dysregulated proliferative states are closely associated with the disruption of the cell cycle regulatory network[27-28]. To gain a deeper understanding of the LHP inhibiting cell proliferation mechanism, flow cytometry was used to analyze the cycle of HepG2 cells after LHP treatment. As the concentration of LHP increased, the number of cells in the G2 phase rose, while those in the S-phase decreased (Figs. 3E and F). Cancer cells in the G2 phase are mainly preparing for the division phase. These results suggested that the inhibitory effect of LHP on HepG2 cells is mainly to prevent the division of cancer cells through the blockage of the G2 phase. The regulation of the cell cycle is mediated by the cyclin-dependent kinases (CDK)/cyclin-dependent kinase inhibitors (CDKI) complex system. In cancer cells, the inactivation or deletion of CDKI factors (e.g., p16, p21, etc.) fails to inhibit CDK activity, resulting in the continuous activation of CDK and subsequent uncontrolled proliferation of cancer cells[29]. The genes of CDKI factors were tested by reverse transcription-quantitative PCR. The results demonstrated the expression of *p15*, *p16*, *p21*, and *p27* were upregulated, and the expression of *p18* was downregulated (Fig. 3G). Among all CDKIs, *p21* exhibited the most significant increase in expression. Elevated levels of p21 can inhibit the activity of CDK4 complexes, thereby preventing cells from entering the S-phase and inhibiting cancer cell proliferation[30-31]. WB assay confirmed an elevation in p21 expression and a decrease in the downstream gene *CDK4* expression at the protein level after LHP intervention (Figs. 3H and I). Thus, these results indicated that LHP intervention modulated the cell cycle by regulating the expression of CDKIs (p21 and CDK4), ultimately leading to the inhibition of HepG2 cell proliferation.

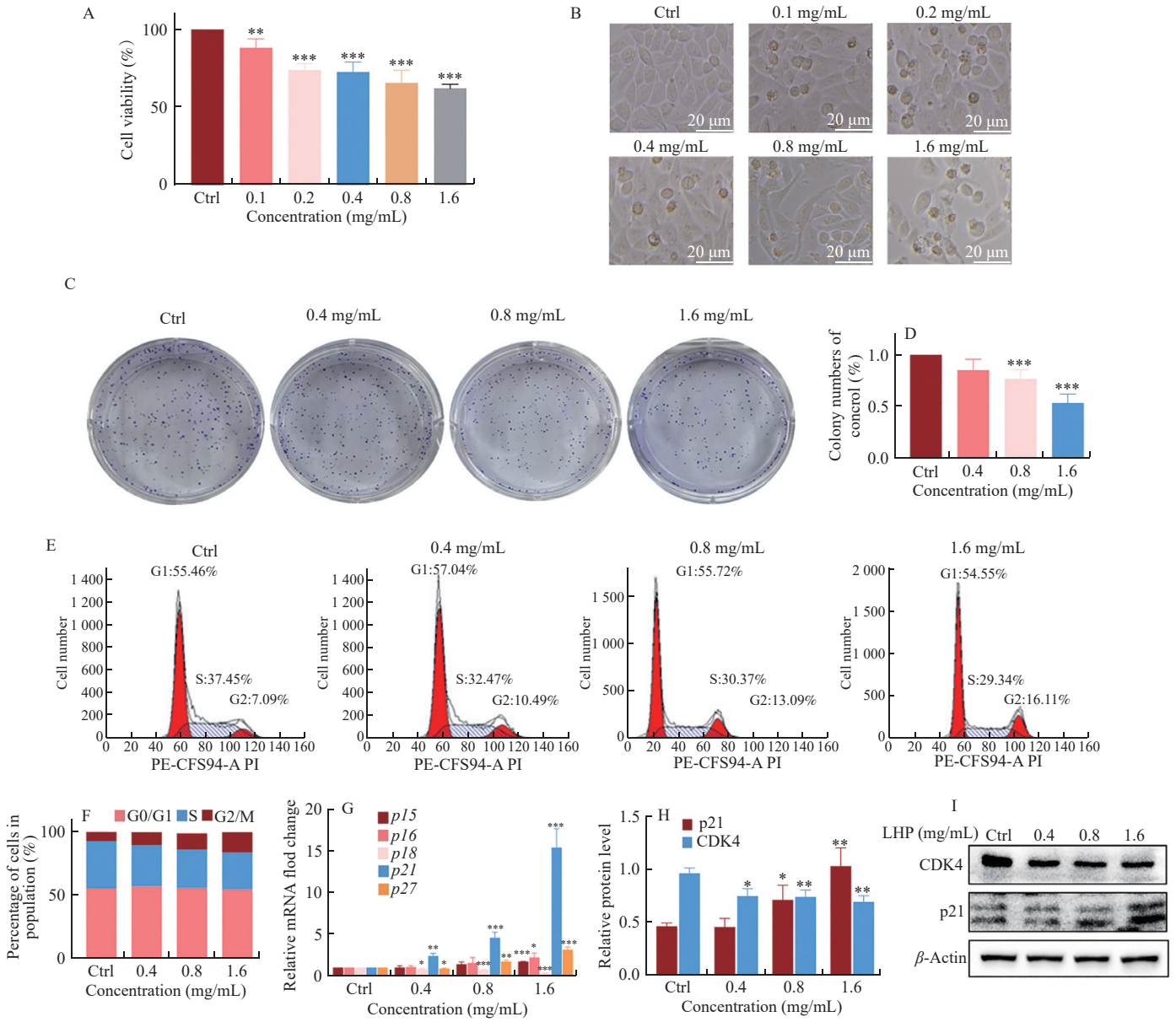

Fig. 3 Inhibition of HepG2 cell proliferation by LHP *in vitro*. (A) Cell viability; (B) cell morphology; (C) crystal violet staining image of bacterial colonies; (D) number of colony; (E and F) cell cycle detected by PI/RNase staining; (G) the relative mRNA expression of *p15, p16, p18, p21*, and *p27*; (H) the relative expression level and (I) WB of p21 and CDK4 protein. Data are presented as mean ± standard error of mean (SEM) of three independent experiments. *** $P < 0.001$, ** $P < 0.01$, * $P < 0.05$.

3.3 The effect of LHP on HepG2 cell apoptosis

In vivo animal models have demonstrated that LHP intervention effectively induced the apoptosis of tumor cells. The quantitative evaluation of apoptosis extent after LHP treatment was assayed using membrane-associated protein V-fluorescein isothiocyanate/PI double staining. The results revealed that the apoptosis rates of HepG2 cells treated with increasing concentrations of LHP (0, 0.1, 0.2, 0.4, 0.8, 1.6 mg/mL) were 0.12%, 0.14%, 2.00%, and 3.40%, respectively (Figs. 4A and B). As the concentration increased, there was a concomitant decrease in the number of normal cells (lower left quadrant), while the number of early apoptotic cells (lower right quadrant), late apoptotic cells (upper right quadrant), and dead cells (upper left quadrant) increased. LHP had the potential to promote HepG2 apoptosis although the initial increase in apoptosis rates may not seem significant ($P > 0.05$). To gain a more visual understanding of apoptosis, the morphology of LHP-treated HepG2 cells was observed by fluorescence microscopy. These analyses revealed the emergence of apoptotic vesicles (Fig. 4C), cytoplasmic swelling, and chromatin condensation, all hallmarks of apoptosis after LHP intervention (Fig. 4D).

The apoptosis in cancer cells primarily occurs through the activation of intrinsic mitochondrial apoptotic pathways mediated by exogenous caspase-8 and death receptors[32-33]. The regulation of intracellular apoptosis is contingent upon the relative levels of anti-apoptotic B-cell leukemia 2 (Bcl-2) and pro-apoptotic Bcl-2-associated X protein (Bax)[34]. Upon receiving apoptotic signals, Bax proteins dimerize, compromising mitochondrial membrane integrity and facilitating the release of pro-apoptotic factors such as cytochrome c[35]. Once in the cytoplasm, cytochrome c binds to

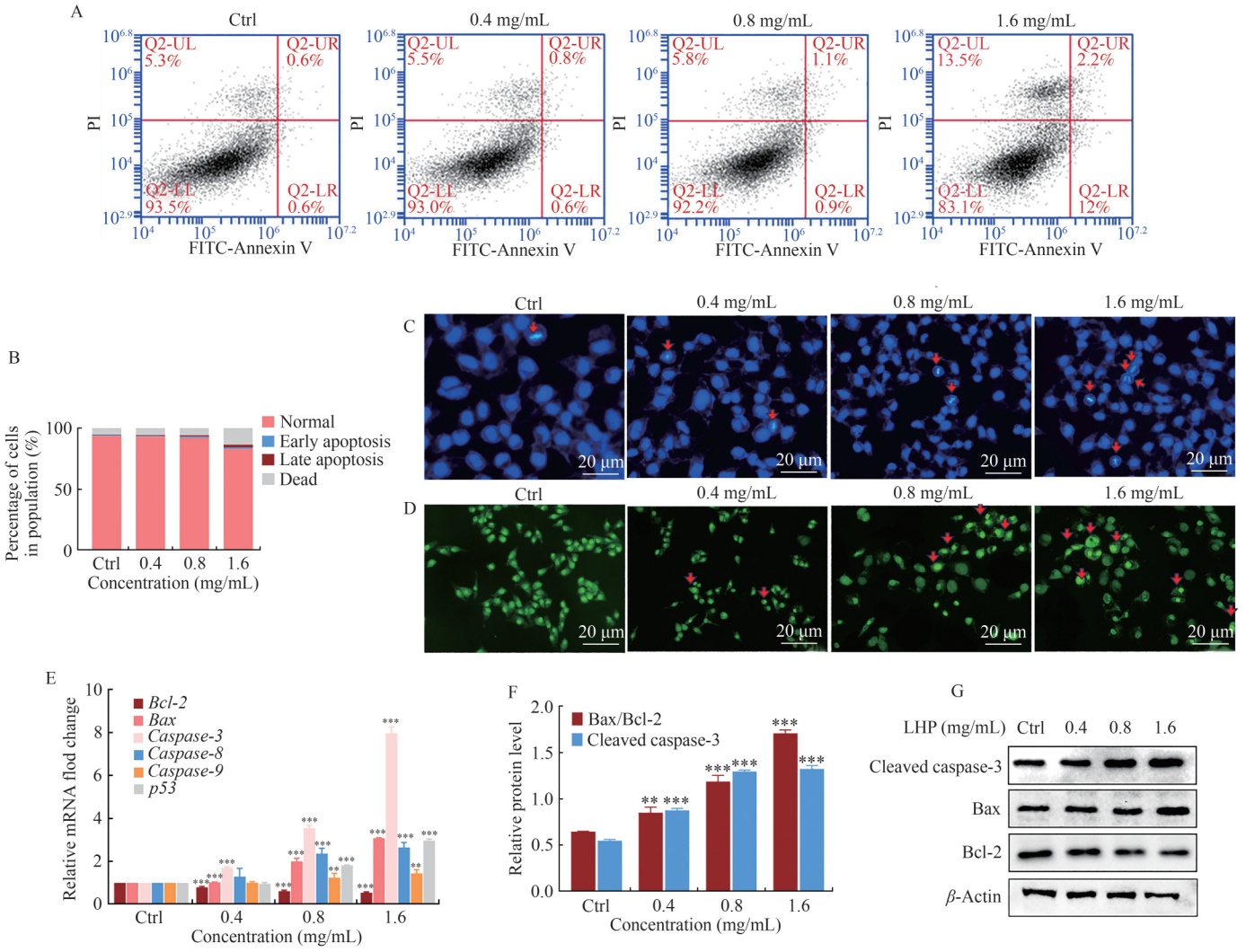

Fig. 4 Promotion of apoptosis in HepG2 cells by LHP *in vitro*. (A) Flow cytometry analysis and (B) the number of cells with different states. (C) Hoechst 33342 staining and (D) acridine orange/ethidium bromide staining were used to observe morphology under a fluorescent microscope. The arrows marked the obvious nuclear shrinkage and the appearance of apoptotic vesicles. (E) The relative mRNA expression levels of *Bax, Bcl-2, caspase-3, caspase-8, caspase-9*, and *p53* were determined by PCR. (F) Bax, Bcl-2, and cleaved caspase-3 proteins were measured by WB, and (G) the relative expression content normalized to *β*-actin was counted. Data are presented as mean ± standard error of mean (SEM) of three independent experiments. *** $P < 0.001$, ** $P < 0.01$.

apoptotic protease activating factor-1 to form the apoptosome. The apoptosome subsequently activates caspase-9. This activation leads to the downstream activation of executor caspases-3, culminating in cell apoptosis[36-37]. The expression of key apoptosis-related genes was detected using both PCR and WB techniques. The results shown in Fig. 4E revealed a significant increase in the Bax/Bcl-2 ratio and cleaved caspase-3, caspase-8, and caspase-9 at the gene level. These findings suggested that LHP promoted the extrinsic apoptosis pathway via caspase-8 and activated the intrinsic apoptosis pathway in mitochondria through the Bcl-2 family, caspase-9, and caspase-3. Consistent with these findings, at the protein level, elevations of the Bax/Bcl-2 ratio and cleaved caspase-3 were also observed with increasing LHP dosages (Figs. 4F and G). This result further demonstrated that LHP can promote apoptosis in HepG2 cells by activating the intracellular mitochondrial apoptotic pathway including Bax and caspase family.

3.4 *The effect of LHP on the invasion ability of HepG2 cell*

Tumor metastasis leading to multiple organ failure is the primary reason for death in cancer patients[38-39]. The metastatic ability of tumor cells is closely related to the ability of tumors to invade surrounding tissues[40-41]. Transwell™ invasion assay was employed to evaluate the invasion ability of cancer cells. A reduction in the invasion rates of cancer cells was observed as the concentration of LHP increased. Specifically, after treating the cancer cells with 1.6 mg/mL of LHP, the invasion rate was significantly reduced to only 45.22% (Figs. 5A and B). These findings suggested that LHP effectively suppresses the invasive capacity of HepG2 cells. Complementing these findings, the scratching experiment further demonstrated that LHP treatment increased the gaps between cell populations in a dosage-dependent manner. Notably, treatment with 1.6 mg/mL of LHP resulted in a 68.02% increase in the gap compared to the control group (Figs. 5C and D). This increase in cell-to-cell spacing

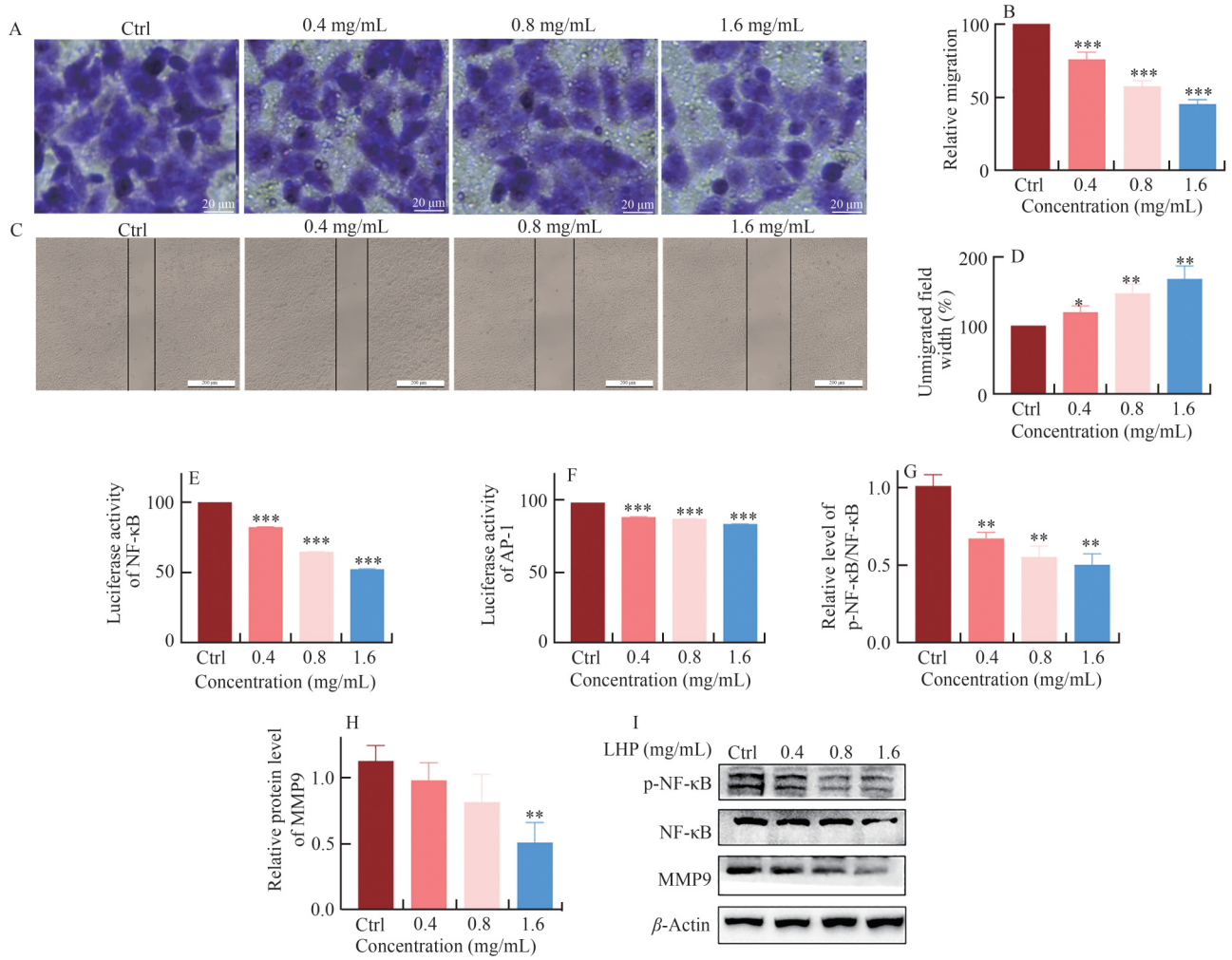

Fig. 5 Inhibition of HepG2 cell migration and invasion by LHP *in vitro*. (A) The invasion after treatment by different concentrations LHP; (B) the cells that passed through the membrane. (C) Cell migration ability and (D) cell counting. Luciferase activity of (E) NF-κB and (F) AP-1. Relative protein levels of (G) p-NF-κB/NF-κB, and (H) MMP9 normalized to *β*-actin. (I) WB of p-NF-κB, NF-κB, and MMP9. Data are presented as mean ± standard error of mean (SEM) of three independent experiments. *** $P < 0.001$, ** $P < 0.01$, * $P < 0.05$.

indicated that LHP also impairs the invasion ability of HepG2 cells.

NF-κB, AP-1, and matrix metalloproteinase-9 (MMP9) exhibit a synergistic interaction in the regulation of cancer cell metastasis[42]. The activation of NF-κB is regulated by the phosphorylation process, which is induced by the NF-κB inhibitor through the action of inhibitory κB kinase. The key component of AP-1 activation is Fos. AP-1 is mainly transcriptionally regulated by serum response factors and ternary complex factors. Despite these different regulatory mechanisms, NF-κB and AP-1 may regulate each other and act synergistically. Specifically, NF-κB and AP-1 function as transcription factors that can enhance the expression of the target gene MMP9. Consequently, MMP9 facilitates the degradation of the extracellular matrix, thereby creating a conducive environment for cancer cell invasion and tumor angiogenesis[43]. The *AP-1* and phospho-*NF-κB* gene expression after LHP intervention was significantly reduced, as shown in Figs. 5E and F. Consistent with this, LHP treatment could effectively suppress the migratory and invasive abilities of HepG2 cells by inhibiting the transcriptional activities of NF-κB and AP-1. The inhibition of NF-κB and AP-1 in turn downregulated the expression of MMP9 (Figs. 5G, H, and I). This mechanism offered a promising approach for targeting tumor metastasis and might hold significant therapeutic potential in cancer treatment.

3.5 Anticancer function of LHP mediated by p53 and NF-κB pathway

p53, as a key tumor suppressor, is precisely activated in response to a variety of stress signals including dysregulated expression of oncogenes[44-45]. For instance, during tumor progression, tissue hypoxia resulting from restricted blood supply could trigger the activation of the *p53* gene[46]. p53 orchestrates various biological responses, such as regulating cell cycle progression, inducing apoptosis, and inhibiting abnormal angiogenesis. Specifically, p53 induces apoptosis in cancer cells by upregulating the expression of the Bax protein. The promotion of Bax subsequently enhances the cleavage activity of caspase-3[47]. Additionally, p53 promotes the expression of the p21 protein. p21 is a crucial negative regulator of the cell cycle by inhibiting the activity of CDK4. This inhibition disrupts the cancer cell cycle, thereby impeding cellular proliferation

(Fig. 6). The p53 pathway-related gene expression was detected using the WB method (Fig. 7). The results revealed that the relative expression of p53 was increased, compared to the control group, which indicated that LHP treatment influenced HepG2 cell proliferation and apoptosis through the p53 pathways.

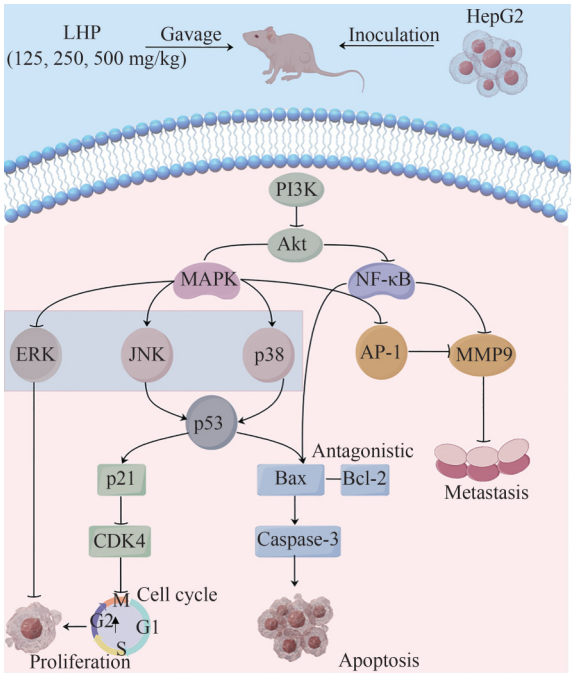

Fig. 6 Schematic diagram of the mechanism of hepatocellular carcinoma inhibition by LHP through p53 and NF-κB signaling pathways. MAPK, mitogen-activated protein kinase; ERK, extracellular regulated protein kinases; JNK, c-Jun N-terminal kinase.

NF-κB is a critical transcription factor involved in the regulation of genes associated with tumor growth, invasion, and metastasis[48-49]. For instance, phosphorylated NF-κB facilitates the transcription and expression of MMP-9 by binding to its promoter region, thereby enhancing tumor cell invasion and metastasis[50]. Additionally, NF-κB influences the apoptotic process by modulating the expression of Bax[51] (Fig. 6). WB analysis (Fig. 7) revealed a reduction in phospho-NF-κB expression, indicating that LHP intervention could inhibit NF-κB activity, thereby exerting anti-cancer effects.

The aberrantly p53 and NF-κB signaling pathways in cancer cells are regulated by the PI3K/Akt signaling pathway. The PI3K/Akt pathway serves as a pivotal regulator of cellular metabolism. PI3K/Akt pathway also is intricately linked to the initiation and progression of various cancers[52]. Specifically, the phosphorylation of PI3K results in the activation of Akt. The phospho-Akt in turn phosphorylates inhibitory κB kinase. This phosphorylation event promotes the degradation of inhibitory κB, leading to the release and activation of NF-κB[53]. Additionally, activated Akt can phosphorylate and activate rapidly accelerated fibrosarcoma kinase (a critical upstream activator in the MAPK signaling pathway), thereby indirectly modulating the p53 signaling pathway[54] (Fig. 6). The activation of MAPK family members can regulate the proliferation, differentiation and death of tumor cells, containing p38, extracellular regulated protein kinases and c-Jun N-terminal kinase[55]. For example, extracellular regulated protein kinase activation by MAPK can directly inhibit cell proliferation. Moreover, p38 and c-Jun N-terminal kinase are also involved in regulating the p53 pathway. As demonstrated by the WB results in Fig. 7, LHP intervention decreased the expression of phosphorylated PI3K, Akt, and extracellular regulated protein kinases, and increased the expression of phosphorylated c-Jun N-terminal kinase and p38 in a dose-dependent manner. These results

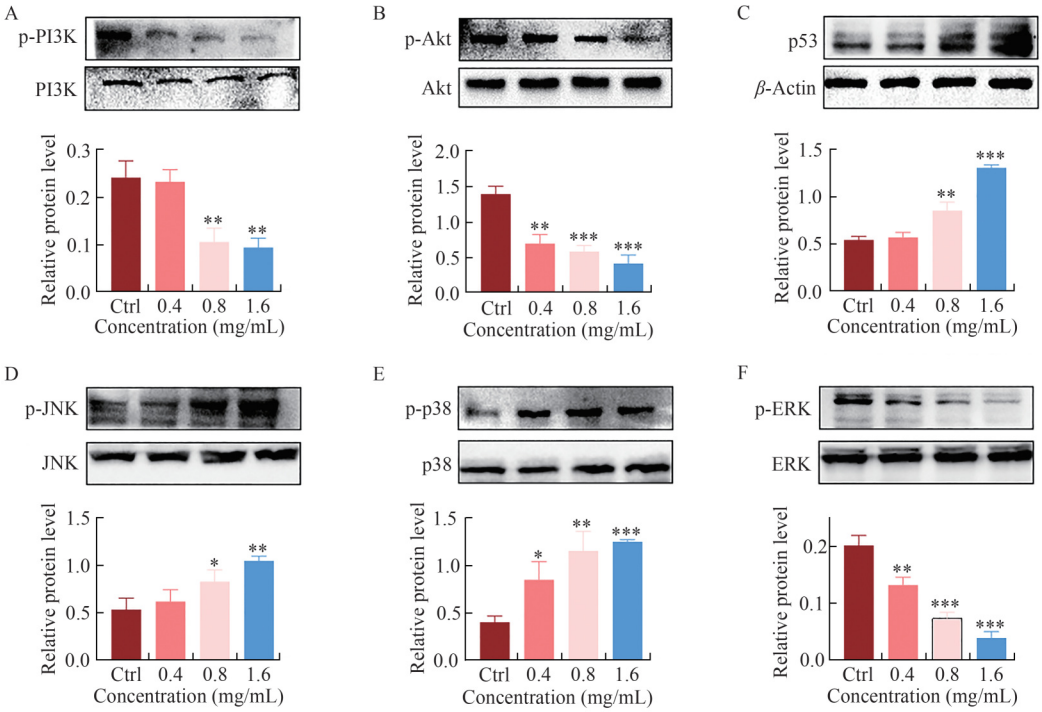

Fig. 7 HepG2 cells were inhibited by LHP *in vitro* through the p53 and NF-κB signaling pathways. (A) p-PI3K, PI3K, (B) p-Akt, Akt, (C) p53, (D) p-JNK, JNK, (E) p-p38, p38, (F) p-ERK, ERK were measured by WB, and the relative expression content normalized to *β*-actin was counted. p-PI3K, phospho-PI3K. Data are presented as mean ± standard error of mean (SEM) of three independent experiments. *** $P < 0.001$, ** $P < 0.01$, * $P < 0.05$.

suggested that LHP could suppress HCC cells by inhibiting the PI3K/Akt signaling pathway.

In conclusion, LHP has exhibited a coordinated and extensive impact on the anti-cancer process through its comprehensive mechanism involving multi-pathway and multi-target actions. This mechanism underscores both the complexity of polysaccharides and potential advantages in anticancer therapy.

3.6 Structure-function relationship

The pharmacological activities of polysaccharides are closely related to chemical structures, encompassing both primary and advanced configurations[4,56]. Previous studies have demonstrated that LHP predominantly consists of three glucans and two galactans[10]. According to existing literature, glucans with *β*-1,3-Glc*p* as the main chain and *β*-1,6-Glc*p* as the branched chain exhibited an enhanced affinity for binding to cell receptors, thereby exerting anticancer effects[9]. Notably, LHP-5 aligned with these structural characteristics. Galactans have demonstrated significant antitumor activity. This was exemplified by the 10 sugar fragments in the synthesized *Panax notoginseng* polysaccharide RN1 served as a crucial functional structure for inhibiting cancer cells[57]. This finding indicated that both LHP-3 and LHP-4 possess potential anticancer properties. Conversely, LHP-1 and LHP-2 exhibited low anticancer activity with *α*-1, 4-Glc*p* as their main chain. However, the *Radix ginseng* Rubra poly saccharide RGRP-1b with a similar structure has been demonstrated to inhibit Huh7 HCC growth through immune regulation[58]. These findings postulated that LHP-1 and LHP-2 may exert anticancer effects via immunomodulation. The results indicated that the multiple structural features of LHP collaborate to produce anticancer effects through various pathways. Investigation of the LHP conformational relationship could elucidate the chemical basis of its anticancer activity and offer a theoretical foundation for target screening and molecular modification of LHP.

4 Conclusion

The anti-HCC effect of LHP extracted from *L. hatsudake* mushroom was studied *in vitro* and *in vivo*, presuming that the mechanism possibly refers to p53 and NF-κB signaling pathways. Furthermore, we found that the anticancer effect of LHP *in vivo* is better than *in vitro*. These findings indicated that whether LHP exerts anticancer effects through immunomodulation deserves to be further studied. Overall, these findings provide a theoretical basis for the further development and application of LHP in adjuvant anti-HCC drugs.

Conflict of interest

There are no conflicts of interest to declare.

Acknowledgements

We gratefully acknowledge the partial support of this research by the Program for Science & Technology Innovation Platform and Talent of Hunan Province (2021RC4032; 2019TP1029), the Key R&D Plan of Hunan Province (2022SK2100; 2023NK2034), the Ministry of Agriculture of the People's Republic of China (GJFP20230204) and the Forestry Science and Technology Innovation Project in Hunan Province (XLK202431).

Appendix A. Supplementary information

Supplementary data associated with this article can be found, in the online version, at http://doi.org/10.26599/FSHW.2024.9250367.

References

[1] H. Sung, J. Ferlay, R.L. Siegel, et al., Global cancer statistics 2020: globocan estimates of incidence and mortality worldwide for 36 cancers in 185 countries, CA. Cancer J. Clin. 71 (2021) 209-249. https://doi.org/10.3322/caac.21660.

[2] P. Tabrizian, G. Jibara, B. Shrager, et al., Recurrence of hepatocellular cancer after resection, Ann. Surg. 261 (2015) 947-955. https://doi.org/10.1097/sla.0000000000000710.

[3] M. Di Maio, E. Basch, J. Bryce, et al., Patient-reported outcomes in the evaluation of toxicity of anticancer treatments, Nat. Rev. Clin. Oncol. 13 (2016) 319-325. https://doi.org/10.1038/nrclinonc.2015.222.

[4] N.Y. Li, C.F. Wang, M.I. Georgiev, et al., Advances in dietary polysaccharides as anticancer agents: structure-activity relationship, Trends Food Sci. Tech. 111 (2021) 360-377. https://doi.org/10.1016/j.tifs.2021.03.008.

[5] H. Teng, L. Chen, Editorial: medicinal plants and their active constituents in the treatment of metabolic syndrome, Front. Pharmacol. 13 (2022) 1031612. https://doi.org/10.3389/fphar.2022.1031612.

[6] Q. Yang, S.L. Chang, X.F. Zhang, et al., The fate of dietary polysaccharides in the digestive tract, Trends Food Sci. Tech. 150 (2024) 104606. https://doi.org/10.1016/j.tifs.2024.104606.

[7] P.R. Guru, R.K. Kar, A.K. Nayak, et al., A comprehensive review on pharmaceutical uses of plant-derived biopolysaccharides, Int. J. Biol. Macromol. 233 (2023) 123454. https://doi.org/10.1016/j.ijbiomac.2023.123454.

[8] W.B. Yu, Y.F. Zhang, L.H. Yao, et al., Research progress on the prevention of tumor by fungal polysaccharides, Trends Food Sci. Tech. 147 (2024) 104422. https://doi.org/10.1016/j.tifs.2024.104422.

[9] G. Chihara, Y. Maeda, J. Hamuro, et al., Inhibition of mouse sarcoma 180 by polysaccharides from *Lentinus edodes* (Berk.) Sing, Nature 222 (1969) 687-688. https://doi.org/10.1038/222687a0.

[10] Q. Yang, S.L. Chang, Y. M. Tian, et al., Glucan polysaccharides isolated from *Lactarius hatsudake* Tanaka mushroom: structural characterization and *in vitro* bioactivities, Carbohydr. Polym. 337 (2024) 122171. https://doi.org/10.1016/j.carbpol.2024.122171.

[11] Y.Q. Liu, Z.Y. Su, O. Tavana, et al., Understanding the complexity of p53 in a new era of tumor suppression, Cancer Cell. 42 (2024) 946-967. https://doi.org/10.1016/j.ccell.2024.04.009.

[12] B. Eluard, C. Thieblemont, V. Baud, NF-κB in the new era of cancer therapy, Trends Cancer 6 (2020) 677-687. https://doi.org/10.1016/j.trecan.2020.04.003.

[13] B. Song, P. Yang, S. Zhang, Cell fate regulation governed by p53: friends or reversible foes in cancer therapy, Cancer Commun. 44 (2024) 297-360. https://doi.org/10.1002/cac2.12520.

[14] H.Q. Shang, X.Y. Niu, W.P. Cui, et al., Anti-tumor activity of polysaccharides extracted from *Pinus massoniana* pollen in colorectal cancer-*in vitro* and *in vivo* studies, Food Funct. 13 (2022) 6350-6361. https://doi.org/10.1039/d1fo03908c.

[15] F. Li, X. Jiao, J. Zhao, et al., Antitumor mechanisms of an exopolysaccharide from *Lactobacillus fermentum* on HT-29 cells and HT-29 tumor-bearing mice, Int. J. Biol. Macromol. 209 (2022) 552-562. https://doi.org/10.1016/j.ijbiomac.2022.04.023.

[16] C.H. Bai, J.Q. Zhao, J.L. Su, et al., Curcumin induces mitochondrial apoptosis in human hepatoma cells through BCLAF1-mediated modulation of PI3K/AKT/GSK-3β signaling, Life Sci. 306 (2022) 120804. https://doi.org/10.1016/j.lfs.2022.120804.

[17] S.S. Narayani, S. Saravanan, J. Ravindran, et al., *In vitro* anticancer activity of fucoidan extracted from *Sargassum cinereum* against Caco-2 cells, Int. J. Biol. Macromol. 138 (2019) 618-628. https://doi.org/10.1016/j.ijbiomac.2019.07.127.

[18] Q. Yang, X.Y. Zhang, H.N. Qin, et al., Phenolic acid profiling of *Lactarius hatsudake* extracts, anti-cancer function and its molecular mechanisms, Foods 11 (2022) 1839. https://doi.org/10.3390/foods11131839.

[19] X.Y. Zhang, S.W. Zhao, X.B. Song, et al., Inhibition effect of glycyrrhiza

polysaccharide (GCP) on tumor growth through regulation of the gut microbiota composition, J. Pharmacol. Sci. 137 (2018) 324-332. https://doi.org/10.1016/j.jphs.2018.03.006.
[20] B.J.A. O'Shaughnessy, R.E. Wittes, G. Burke, et al., Commentary concerning demonstration of safety and efficacy of investigational anticancer agents in clinical trials, J. Clin. Oncol. 9 (2019) 2225-2232. https://doi.org/10.1200/JCO.1991.9.12.2225.
[21] Y. Zhou, M. Zhang, Z.L. Zhang, et al., Hydrazinocurcumin and 5-fluorouracil enhance apoptosis and restrain tumorigenicity of HepG2 cells via disrupting the PTEN-mediated PI3K/Akt signaling pathway, Biomed. Pharmacother. 129 (2020) 109851. https://doi.org/10.1016/j.biopha.2020.109851.
[22] S. Zong, J.L. Li, L. Yang, et al., Mechanism of bioactive polysaccharide from *Lachnum* sp. acts synergistically with 5-fluorouracil against human hepatocellular carcinoma, J. Cell. Physiol. 234 (2019) 15548-15562. https://doi.org/10.1002/jcp.28202.
[23] F. Fontana, P. Figueiredo, J.P. Martins, et al., Requirements for animal experiments: problems and challenges, Small 17 (2020) 1-8. https://doi.org/10.1002/smll.202004182.
[24] S. Harloff-Helleberg, L.H. Nielsen, H.M. Nielsen, Animal models for evaluation of oral delivery of biopharmaceuticals, J. Control. Release 268 (2017) 57-71. https://doi.org/10.1016/j.jconrel.2017.09.025.
[25] J.C. Li, H.L. Wang, L. Wang, et al., Decursin inhibits the growth of HepG2 hepatocellular carcinoma cells via Hippo/YAP signaling pathway, Phytother. Res. 32 (2018) 2456-2465. https://doi.org/10.1002/ptr.6184.
[26] S.C. Yang, C.D. Hu, X.M. Chen, et al., Crosstalk between metabolism and cell death in tumorigenesis, Mol. Cancer 23 (2024) 71. https://doi.org/10.1186/s12943-024-01977-1.
[27] A.M. Intlekofer, L.W.S. Finley, Metabolic signatures of cancer cells and stem cells, Nat. Metab. 1 (2019) 177-188. https://doi.org/10.1038/s42255-019-0032-0.
[28] L.G. Zhu, J. Wang, Quantifying landscape-flux via single-cell transcriptomics uncovers the underlying mechanism of cell cycle, Adv. Sci. 11 (2024) 2308879. https://doi.org/10.1002/advs.202308879.
[29] M. Salvadores, F. Supek, Cell cycle gene alterations associate with a redistribution of mutation risk across chromosomal domains in human cancers, Nat. Cancer 5 (2024) 330-346. https://doi.org/10.1038/s43018-023-00707-8.
[30] A.L. Gartel, S.K. Radhakrishnan, Lost in transcription: p21 repression, mechanisms, and consequences, Cancer Res. 65 (2024) 3980-3985. https://doi.org/10.1158/0008-5472.can-04-3995.
[31] Z.C. Tong, Y.B. Zhao, S.Y. Bai, et al., The mechanism of resistance to CDK4/6 inhibition and novel combination therapy with RNR inhibition for chemo-resistant bladder cancer, Cancer Commun. 44 (2024) 700-704. https://doi.org/10.1002/cac2.12532.
[32] Y.W. Ai, Y.T. Meng, B. Yan, et al., The biochemical pathways of apoptotic, necroptotic, pyroptotic, and ferroptotic cell death, Mol. Cell. 84 (2024) 170-179. https://doi.org/10.1016/j.molcel.2023.11.040.
[33] Y.H. Wu, S.T. Mo, I.T. Chen, et al., Caspase-8 inactivation drives autophagy-dependent inflammasome activation in myeloid cells, Sci. Adv. 8 (2022) 1-18. https://doi.org/10.1126/sciadv.abn9912.
[34] X.R. Chang, S.Y. Niu, M.T. Shang, et al., ROS-Drp1-mediated mitochondria fission contributes to hippocampal HT22 cell apoptosis induced by silver nanoparticles, Redox. Biol. 63 (2023) 102739. https://doi.org/10.1016/j.redox.2023.102739.
[35] Y. Chen, J.R. Yang, Y. Zuo, et al., Voacamine is a novel inhibitor of EGFR exerting oncogenic activity against colorectal cancer through the mitochondrial pathway, Pharmacol. Res. 184 (2022) 106415. https://doi.org/10.1016/j.phrs.2022.106415.
[36] Z.W. Zhang, L.H. Hou, D. Liu, et al., Directly targeting BAX for drug discovery: therapeutic opportunities and challenges, Acta. Pharm. Sin. B. 14 (2024) 2378-2401. https://doi.org/10.1016/j.apsb.2024.02.010.
[37] J.Y. Yuan, D. Ofengeim, A guide to cell death pathways, Nat. Rev. Mol. Cell. Biol. 25 (2023) 379-395. https://doi.org/10.1038/s41580-023-00689-6.
[38] G. Bergers, S.M. Fendt, The metabolism of cancer cells during metastasis, Nat. Rev. Cancer 21 (2021) 162-180. https://doi.org/10.1038/s41568-020-00320-2.
[39] S.L. Liu, W. Dai, B. Jin, et al., Effects of super-enhancers in cancer metastasis: mechanisms and therapeutic targets, Mol. Cancer 23 (2024) 122. https://doi.org/10.1186/s12943-024-02033-8.
[40] M. Castaneda, P. den Hollander, N.A. Kuburich, et al., Mechanisms of cancer metastasis, Semin. Cancer Biol. 87 (2022) 17-31. https://doi.org/10.1016/j.semcancer.2022.10.006.
[41] Y.J. Zhou, M.L. Yang, X. He, et al., RNA-binding protein RPS7 promotes hepatocellular carcinoma progression via LOXL2-dependent activation of ITGB1/FAK/SRC signaling, J. Exp. Clin. Cancer Res. 43 (2024) 45. https://doi.org/10.1186/s13046-023-02929-1.
[42] M.A. Karreman, A.T. Bauer, G. Solecki, et al., Active remodeling of capillary endothelium via cancer cell-derived MMP9 promotes metastatic brain colonization, Cancer Res. 83 (2023) 1299-1314. https://doi.org/10.1158/0008-5472.Can-22-3964.
[43] Q. Sun, Z. Yang, P. Li, et al., A novel miRNA identified in GRSF1 complex drives the metastasis via the PIK3R3/AKT/NF-κB and TIMP3/MMP9 pathways in cervical cancer cell, Cell. Death Dis. 10 (2019) 636. https://doi.org/10.1038/s41419-019-1841-5.
[44] Y.M. Huang, Z.H. Jiao, Y.Q. Fu, et al., An overview of the functions of p53 and drugs acting either on wild- or mutant-type p53, Eur. J. Med. Chem. 265 (2024) 116121. https://doi.org/10.1016/j.ejmech.2024.116121.
[45] W.L. Liu, X.X. Li, E.S.H. Chu, et al., Paired box gene 5 is a novel tumor suppressor involved in the pathogenesis of hepatocellular carcinoma through interaction with p53 signaling pathway, Gastroenterology 140 (2011) 145. https://doi.org/10.1016/s0016-5085(11)60589-1.
[46] Y.F. Qian, C.Y. Shi, C. Cheng, et al., Ginger polysaccharide UGP1 suppressed human colon cancer growth via p53, Bax/Bcl-2, caspase-3 pathways and immunomodulation, Food Sci. Hum. Well. 12 (2023) 467-476. https://doi.org/10.1016/j.fshw.2022.07.048.
[47] D.J. Turnham, H. Smith, R.W.E. Clarkson, Suppression of bcl3 disrupts viability of breast cancer cells through both p53-dependent and p53-independent mechanisms via loss of NF-κB signalling, Biomedicines 12 (2024) 142. https://doi.org/10.3390/biomedicines12010143.
[48] Y.F. Li, B.W. Zhao, J.Z. Peng, et al., Inhibition of NF-κB signaling unveils novel strategies to overcome drug resistance in cancers, Drug Resist. Update 73 (2024) 101042. https://doi.org/10.1016/j.drup.2023.101042.
[49] Y. Chiu, A. Husain, K.M. Sze, et al., Midline 1 interacting protein 1 promotes cancer metastasis through FOS-like 1-mediated matrix metalloproteinase 9 signaling in HCC, Hepatology 78 (2023) 1368-1383. https://doi.org/10.1097/hep.0000000000000266.
[50] Y.X. Yang, S.S. Song, S.J. Li, et al., GATA4 regulates the transcription of MMP9 to suppress the invasion and migration of breast cancer cells via HDAC1-mediated p65 deacetylation, Cell. Death Dis. 15 (2024) 289. https://doi.org/10.1038/s41419-024-06656-z.
[51] N.Z. Shaban, A.A. El-Faham, M.M. Abu-Serie, et al., The black *Vitis vinifera* seed oil saponifiable fraction ameliorates hepatocellular carcinoma *in vitro* and *in vivo* via modulating apoptosis and ROS/NF-κB signaling, Biomed. Pharmacother. 171 (2024) 116215. https://doi.org/10.1016/j.biopha.2024.116215.
[52] Y. He, M.M. Sun, G.G. Zhang, et al., Targeting PI3K/Akt signal transduction for cancer therapy, Signal. Transduct. Tar. 6 (2021) 425. https://doi.org/10.1038/s41392-021-00828-5.
[53] J. Leng, H.Y. Li, Y.Q. Niu, et al., Low-dose mono (2-ethylhexyl) phthalate promotes ovarian cancer development through PPARα-dependent PI3K/Akt/NF-κB pathway, Sci. Total. Environ. 790 (2021) 147990. https://doi.org/10.1016/j.scitotenv.2021.147990.
[54] V. Ramalingam, N. Narendra Kumar, M. Harshavardhan, et al., Chemical profiling of marine seaweed *Halimeda gracilis* using UPLC-ESI-Q-TOF-MSE and evaluation of anticancer activity targeting PI3K/AKT and intrinsic apoptosis signaling pathway, Food Res. Int. 157 (2022) 111394. https://doi.org/10.1016/j.foodres.2022.111394.
[55] V.K. Singh, D. Arora, N.K. Satija, et al., Intricatinol synergistically enhances the anticancerous activity of cisplatin in human A549 cells via p38 MAPK/p53 signalling, Apoptosis 22 (2017) 1273-1286. https://doi.org/10.1007/s10495-017-1404-0.
[56] X.Y. Guo, J. Kang, Z.Y. Xu, et al., Triple-helix polysaccharides: formation mechanisms and analytical methods, Carbohydr. Polym. 262 (2021) 117962. https://doi.org/10.1016/j.carbpol.2021.117962.
[57] X.J. Qin, C.H. Xu, M.L. Liu, et al., Synthesis of branched arabinogalactans up to a 140-mer from *Panax notoginseng* and their anti-pancreatic-cancer activity, Nat. Synth. 3 (2024) 245-255. https://doi.org/10.1038/s44160-023-00428-x.
[58] X.Y. Zhang, Z.J. Liu, C. Zhong, et al., Structure characteristics and immunomodulatory activities of a polysaccharide RGRP-1b from *Radix ginseng* Rubra, Int. J. Biol. Macromol. 189 (2021) 980-992. https://doi.org/10.1016/j.ijbiomac.2021.08.176.